Electron Spectrometer for multi-GeV Laser-Plasma accelerator

Nadejda Drenska and Riccardo Faccini
Sapienza University, Rome, Italy.

Claudio Gatti
LNF INFN, Frascati (RM), Italy.

Silvia Martellotti*
LNF INFN, Frascati (RM) and Roma Tre University, Rome, Italy

Paolo Valente
Sapienza University and INFN Roma1, Rome, Italy.

(PlasmonX Collaboration)
(Dated: March 13, 2012)

The upcoming laser plasma acceleration PlasmonX experiments, with the 250 TW laser at the FLAME facility of the INFN Laboratori Nazionali di Frascati, pushes the regime of the resulting accelerated particles to higher energies and intensities, entering in the GeV regime with more than 100 pC of electrons. At the current status of understanding of the acceleration mechanism, relatively large angular and energy spreads are expected. There is therefore the need for developing a device capable of measuring electron energies over three orders of magnitude (few MeV to few GeV) of bunches with still unknown angular divergence. A spectrometer is being constructed to perform these measurements. It is made of an electro-magnet and a screen made of scintillating fibers for the measurement of the trajectories of the particles. The large range of operation, the huge number of particles and the need to focus the divergence, present challenges in the design and construction of such a device. We present the design of this spectrometer that lead to the use of scintillating fibers, multichannel photo-multipliers and a multiplexing electronics, a combination which is innovative in the field. We also present the experimental results obtained on a prototype with the high intensity electron beam at the LNF beam test facility and the preliminary results of the commissioning phase.

PACS 52.38.Kd: Laser-plasma acceleration of electrons and ions

PACS 29.40.Mc: Scintillation detectors

PACS 07.81.+a: Electron and ion spectrometers

I. INTRODUCTION

Laser-plasma interaction is a new technique for charged particle acceleration. The idea of using focused laser beams to excite a longitudinal plasma wave to accelerate particles was first proposed by Tajima e Dawson in 1979 [1]. Due to its ponderomotive force, a laser pulse crossing a plasma generates an electron wake wave. The intense electric fields associated to this plasma wave are able to accelerate high energy particles [2]. Energy and characteristics of the produced accelerated bunch strongly depends on the laser parameters and the plasma density.

At the Frascati National Laboratory (LNF) the last generation laser FLAME (Frascati Laser for Acceleration and Multidisciplinary Experiments) has been realized in order to provide ultra-short laser pulses, with length of 20 fs, peak-power up to 300 TW and intensity of $10^{18}\, W/cm^2$ with a repetition rate of 10 Hz. The first step of PlasmonX project is a Self Injection Test Experiment (SITE) [3]: The laser FLAME is focused on a 4 mm gas-jet layer with the goal of producing sub-Gev-class electron bunches from laser-plasma interaction.

A 3D simulation has been performed, for plausible laser and plasma parameters, with the PIC code ALaDyn [5]. Fig. 1 shows the expected energy for the accelerated electron bunch: the whole spectrum is spread from a few MeV to slightly less than 1 GeV. The electron charge of the high energy peak is of the order of 10^9 particles. Fig. 2 shows the expected angular divergence relative to this accelerated bunch.

The realization of a magnetic spectrometer for the detection of this bunch represents a challenge because it must measure the energy spectrum of tens of millions of particles, arriving simultaneously, spread over three order of magnitudes in momentum, coming from a point-like source about a meter upstream, with a divergence of some mrad.

* silvia.martellotti@lnf.infn.it

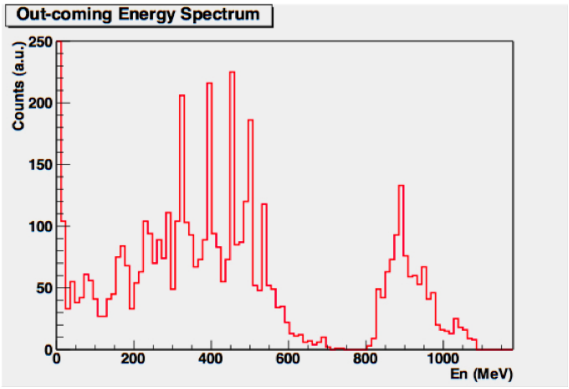

FIG. 1. Energy spectrum for the electron bunch as expected from a 3D PIC ALaDyn simulation [5].

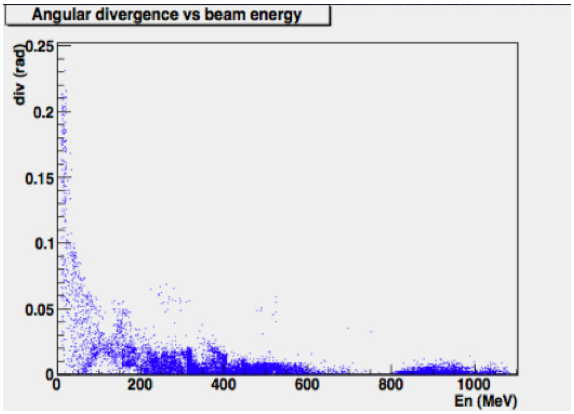

FIG. 2. Angular divergence for the electron bunch as expected from a 3D PIC ALaDyn simulation [5].

II. SPECTROMETER DESIGN

The spectrometer is composed by a dipole electromagnet deflecting charged particles and a scintillating fiber position detector placed inside a vacuum chamber [6], the technical drawing is shown in Fig. 3. The aim is to reach 1% resolution in the widest possible momentum range.

The dipole in use for the first step of the PlasmonX project can generate a magnetic field of 0.45 T on a 6 cm gap over a lenght of 20 cm. With this magnet a resolution better than 1% is guaranteed up to 200 MeV. An upgrade of the spectrometer using a magnet with three times the magnetic field and twice the length of the poles is being designed. With the upgraded magnet the 1% resolution will be extended up to energies greater than 1 GeV.

The active part of the detector is composed by an array of Kuraray SCSF-81 single-cladding scintillating fibers with 1.00 $\pm$ 0.05 mm diameter. The core material is polystyrene with refractive index $n_{co} = 1.59$, while the cladding material is polymethylmethacrylate with refractive index n_{cl}=1.49; the trapping efficiency is 3.1%. The nominal attenuation length is about 3.5 m. The emission peak is in the blue region at 437 nm. The fibers are enclosed in an aluminum vacuum chamber through a long aperture in the top part of the chamber, sealed with epoxy glue. The height of the vacuum chamber is driven by the size of the gap between the magnet's poles (6 cm), while the total length of the detector, and thus of the vacuum chamber, is dictated by the available space between the gas-jet, i.e. the laser-plasma interaction point, and the wall of the experimental hall (setup details are in [3]).

The principle of the momentum reconstruction is the classic one: charged particles with different momentum values are dispersed in the uniform magnetic field generated by the dipole with a bending radius dependent on their momentum. Particle energy can be then determined by measuring the impact point on an appropriately shaped detector.

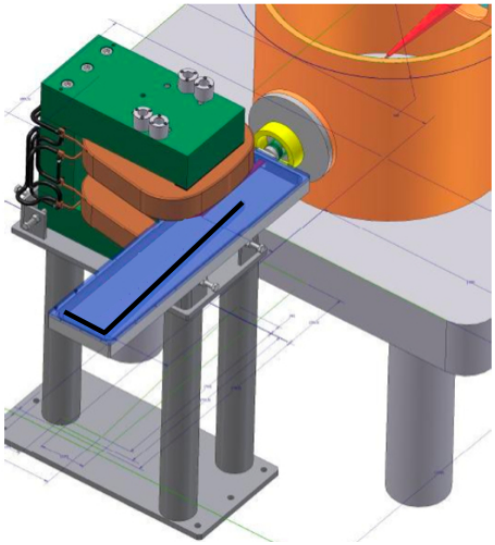

FIG. 3. Technical drawing of the spectrometer: the vacuum chamber (blue), inserted between the poles (orange) of the magnet (green). In black the active part of the fiber detector.

A. Magnet and detector geometry

The resolution is dominated by the beam angular divergence [4]: trajectories from signifcantly different momenta could be overlaid on the same position on the detector. The detector geometry has been studied in order to focalize as much as possible in the same position the electrons with the same energy but different unknown angular divergence.

If electrons enter the dipole close to the edge, where the field has a strong variation, the deflection will be strongly dependent on the distance of the trajectory from the magnetic center. In this "fringe" area, particles going towards the center of the magnet will undergo a higher bending power, with respect to particles with the same energy but a more external trajectory: this turns out in

a focusing effect, even though the total deflection will be smaller since the field integral will not be the design one.

The optimum configuration with the present magnet (B_{max}=0.45 T) is shown in Fig. 4: particles cross the magnet 13 cm off the center obtaining a focusing effect for energies up to 200 MeV. The position sensitive detector is split in two parts, one placed on the focal plane for the low-momentum particles (Low det); and one for electrons of more than 200 MeV (High det) placed in the forward direction, orthogonally to the laser beam propagation direction, as far as possible from the magnet in order to maximize the spread for different energies.

This setup should provide the demanded energy resolution ($< 1\%$) up to 200 MeV and a poorer resolution ($< 5\%$) up to almost 1 GeV. To achieve a resolution $< 1\%$ up to 1 GeV and above, the spectrometer will be upgraded.

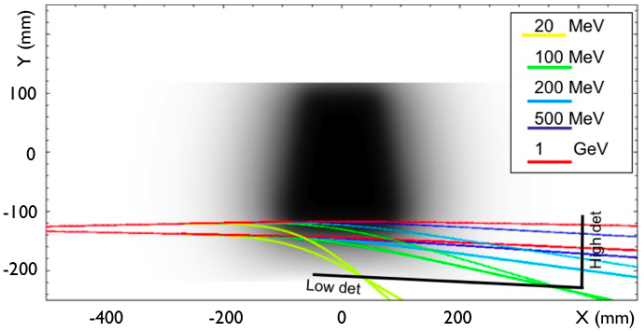

FIG. 4. Top view of the spectrometer set-up: the dark part is the density plot of the magnetic field; the two black lines indicate the detectors; trajectories for different energies are evaluated.

B. Detection and readout technology

The scintillating fibers allow the propagation of the photons generated by the ionizing electrons through scintillating process inside the fiber core to the sensitive area of photomultiplier tubes.

The intrinsic detector granularity given by fiber dimension, has a negligible effect on the resolution. Having fixed the geometry of the sensitive area, the granularity contribution to the resolution has been studied. In the low-momentum detector, thanks to the simultaneous effect of focussing and of the large deflection, a detector resolution of a few millimeters (more than one fiber) is sufficient to keep the resolution below the 1% level over the whole momentum range (20÷200 MeV). In the high-momentum detector, the small deflection seems to require a higher granularity, however the dominant contribution to the momentum resolution is given by the angular dispersion, for a beam divergence of a few mrad, a resolution much better than 1 mm would not give a significant improvement.

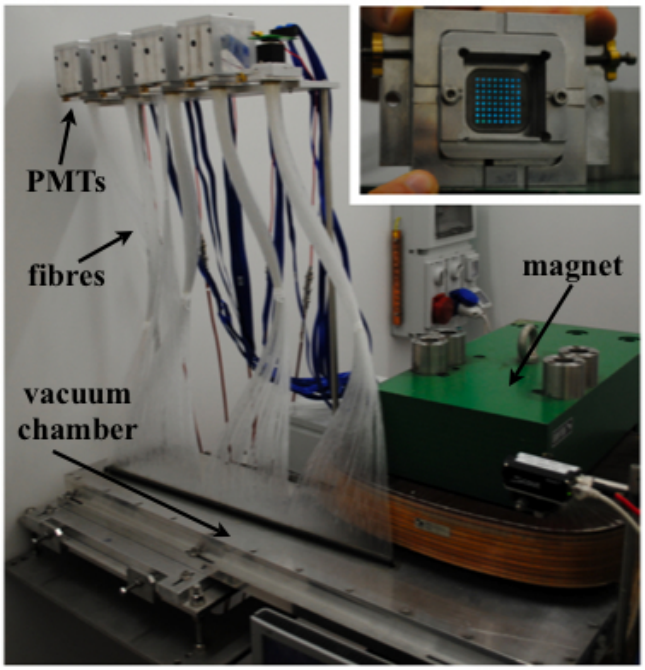

FIG. 5. Spectrometer components. The PMT are inside aluminum boxes for light-tightness and electromagnetic shielding. The fiber bundles enter the vacuum chamber through the visible black flange. On the top right view of the fibers mask, with the PMT adjustable holder, the two-dimensional movement can be achieved by means of precision screws.

Scintillating fibers have been chosen because they are flexible and easy to be arranged in the desired shape, can cover large sensitive areas, are essentially blind to photons and can be coupled to the photo-detector at some distance, outside the vacuum, without significant loss of light, and without any carefully aligned optical system. One drawback is that one readout channel per fiber is needed.

The fibers are grouped in bundles and coupled to pcoupled to the photodetectors: 8×8 multi-anode Hamamatsu photomultiplier H7546B (R7600-00). The anode size is 2×2 mm^2 with a total effective area of 18.1×18.1 mm^2. The typical cross-talk between pixels, about 2% is adequate for our purposes. The coupling between the fibers and the PMT is realized with a precision machine-drilled metal mask into which the fiber's extremities are glued, using an optical cement (Bicron BC-400 from Saint-Gobain).

Up to now, in laser-plasma acceleration experiments, only optical devices have been used. Segmented-anode photomultipliers have been chosen, mainly considering the possibility of adjusting the sensitivity of the detector to a very wide range of beam intensities. Photomultiplier tubes (PMT) can indeed reach gain values as high as 10^6, and thus be sensitive to single photo-electrons, but they can as well be efficiently operated at much lower gains, down to the 10^2 range.

The picture in fig. 5 shows the vacuum chamber, the

fibers exiting from it, and the five fiber bundles going to coupling masks where the PMT's are installed and cabled to the electronics.

Since a few mm resolution is more than enough in the low-momentum detector, in order to reduce the number of readout channels we couple 3 fibers to a single PMT channel, and we read only 3 out of 4 fibers, while we keep a one to one correspondance for the high-momentum detector. We end up with 192 channels in the low-momentum region, covering a sensitive length of 768 mm, and 128 in the high-momentum region, covering 128 mm. This configuration requires the use of three 64-channels PMT's in the low-momentum detector and two in the high-momentum one.

The readout of the 320 channels is performed simultaneously by a front-end electronics system designed for PET/SPECT detectors using multi-anode PMT's and up to 4096 channels. The system is based on MAROC2 chips (Multi Anode ReadOut Chip) developed in LAL, Orsay [7]. The MAROC2 chip amplifies and shapes the analog input signals, sample and holds them, and then feeds them to a 10-bit Wilkinson ADC multiplexing the 64 channels. The gain of the amplifier and shaping stage can be adjusted from 4 to 0.25 with 6 bits resolution. This also gives an handle to adjust the dynamic range of our instrument to the beam charge. The data are recorded and shown online event by event.

In order to further extend the dynamic range, and to reduce the possibility of having saturation of the detector's response to very high-charge beams, the possibility of interposing a neutral-density optical filter (NDF) between the scintillating fibers mask, and the surface of the PMT, in order to attenuate the light by a known factor A_{NDF} is foresee.

The total charge Q is a funcion of the amplitude measured by our acquisition system, A_{meas}:

$$A_{meas} \propto N \times n_{ph.el.} \times A_{NDF} \times G_{PMT} \times g \qquad (1)$$

where N is the number of electrons impacting the fibers, $n_{ph.el.}$ the number of photo-electrons generated for each particle (including the fibers' efficiency and attenuation, the optical coupling to the photomultiplier and its quantum efficiency), G_{PMT} the gain of the PMT, and g the gain of the electronics.

The function $Q = Q(A_{meas})$ is found by calibration.

C. Data Analysis

The reconstruction of the momentum distribution starting from the position measurement is realized with a Bayesian Unfolding [9]. This method is based on the estimate of $P(p|i)$ (probability distribution of the momentum p if a given fiber i is hit) with the Bayes theorem:

$$P(p|i) = \frac{P(i|p) \times P(p)}{\sum_{p'} P(i|p') \times P(p')} \qquad (2)$$

where $P(i|p)$ is the detector response and $P(p)$ is the a-priori momentum distribution. A flat probability in the energy range from 0 to 1.6 GeV has been chosen.

The *detector response* $P(i|p)$ was studied using a Geant4 based simulation that takes into account the experimental set-up and the measured magnetic field. Beam bunches with 2 mrad gaussian divergence with energies from 0 to 1.6 GeV were simulated. The result is the smearing matrix $P(i|p)$ that can be summarized in a 2D histogram, shown in Fig. 6, where the x axis represents the momentum and the y axis represents the fibers. The area of each box is proportional to the probability $P(i|p)$ of the momentum p to release signal in fiber i.

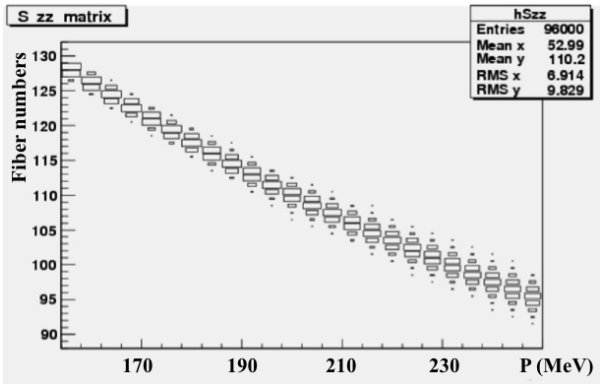

FIG. 6. Smearing matrix of the $P(i|p)$ obtained by a Geant4 simulation of the detector response.

The number of electrons with momentum p (their charge $\hat{Q}_p$) is evalueated from the charge Q_i deposited in the $i-$th fiber:

$$\hat{Q}_p = \sum_i Q_i \times P(p|i) \qquad (3)$$

Once specified the $P(i|p)$ matrix, the Bayesian unfolding only needs in input the observed electron position distribution given by the 320 electronic signals. The resolution obtained with this method vs energy is shown in Fig. 7 for 1 iteration (red) and 10 iterations (green) of the unfolding procedure.

III. PROTOTYPE TEST AND ABSOLUTE CALIBRATION

In order to test the entire readout chain and to perform an absolute calibration of the fiber detector, a prototype of 64 scintillating fibers read by a single H7546B PMT has been made up and different sets of test have been performed, using the electron beam provided by the Frascati Beam Test Facility (BTF)[10], in order to calibrate the detector and find the optimal working point.

Prototype test are performed with electron beams of 500 MeV and charges from the pC up to the nC range. The beam charge is measured by an Integrating Current Transformer (ICT) toroid (Bergoz, 10:1 transformer

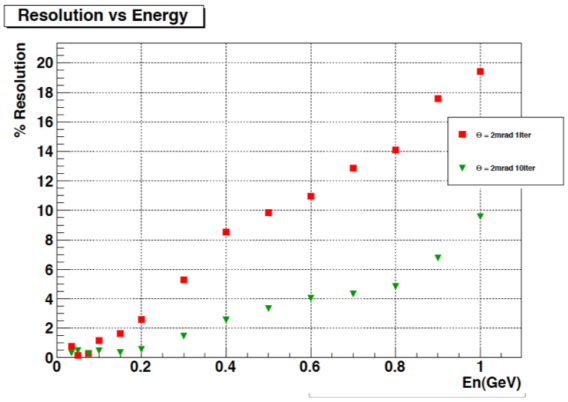

FIG. 7. Energy resolution obained with 1 (red) and 10 (green) iterations of the Bayesian unfolding.

ratio, 30 ns risetime), and the beam-spot independently measured by means of a high-fluorescence flag readout by a videocamera. The scintillating fiber of the prototype are placed perpendicularly to the electron beam, and readout by our standard MAROC electronics. The profile of the beam was clearly visible and compatible with the measured beam-spot. In this configuration the linearity of the gain curve of the PMT and of the MAROC electronics have been studied, and the response of the detector with high beam charges was calibrated . For this purpose, a neutral density filter with attenuation factor $A_{NDF} = 0.4\%$ has been used. In this configuration we were able to perform a calibration up to 0.5 nC, and we observed a good linearity up to ≈ 0.2 nC, as shown in fig.8. The PMT and electronic gains can be tuned in order to avoid saturation effects. Optimal values of these parameters have been found.

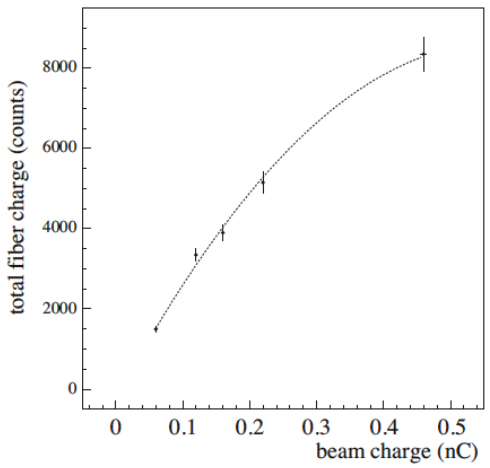

FIG. 8. Calibration of the fiber detector signal as a function of the beam charge measured by the ICT, with 500 MeV electrons from the BTF line.

In addition also the magnet fringe field focusing property has been tested at BTF. For a fixed electron energy of about 250 MeV, the beam position before and after the propagation inside the spectrometer magnet has been observed. The initial beam had a Gaussian shape with a spot size of the order of a few mm. The expectations of the focusing in the fringe field have extensively checked, measuring the beam spot size variations as a function of the position and angle of the beam entrance point in the magnet. The measured spot size versus distance of the beam axis from the magnetic center is shown in Fig. 9. Only statistical error of the gaussian fit are reported in figure, systematic errors, increasing for low magnet intensities, have not been deeply studied but the focusing effect is clearly demostrated.

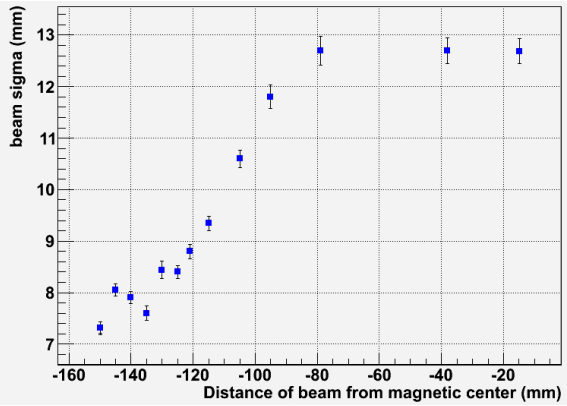

FIG. 9. Spot size measurement vs distance of the beam axis from the magnet center.

IV. COMMISSIONING

The commissioning phase has now started and first electron bunches have been accelerated with low laser intensity and preliminarly experimental condition. Unfortunately the readout electronics suffered from the electromagnetic noise induced by the pulsed high energy field generated in the laser-plasma interaction, making it impossible to discriminate signal from noise. It is worth to stress once again that this was the first attempt of using a not purely optical device in a laser-plasma interaction environment. The most challenging part of the system is indeed the use of photodetectors in a high-noise environment, with both electromagnetic shots and bursts of Xrays directly on multi-pixel photomultipliers.

To reduce the noise the following measures have been taken:

- extend fiber length from 1 to 3 meter, in order to place PMTs and electronics behind the radiation protection wall of the experimental area. Moreover the consequent increase of light attenuation is an advantage against saturation effects;
- attenuate the signal at the entrance of the MAROC2 chips with customized attenuators en-

suring an appropriate interface with our electronics.

- revise the grounding of the whole system;

- realize Faraday cages with μmetal instead of anodized aluminum, for screening the PMTs and electronics.

These improvements will be tested as soon as the commissioning resumes.

At the same time an alternative optical readout system was realized to estimate the light emitted from the scintillating fibers, making use of CCD cameras. The intensity of the light outgoing from the fibers was registered. The signal is proportional to the impacting electron charge and this metod permitted to analyse the accelerated electrons bunches.

One of the resulting distributions of the fiber signals as placed on the detector is shown in Fig.10. Fig.11 shows the corresponding unfolded energy spectrum. The shape is characterized by a broad distribution at low energies and a long tail above 100 MeV. Such a low energy spectrum is due to the low laser pulse intensity used in this first attempt and a not yet optimized laser-plasma interaction setup.

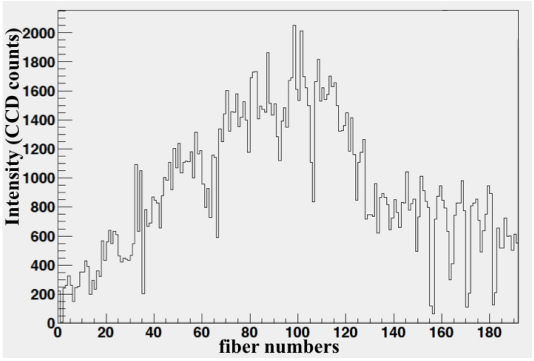

FIG. 10. CCD counts versus fiber position.

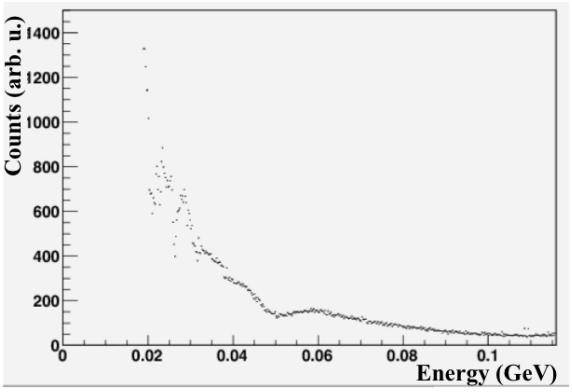

FIG. 11. Example of a broad energy spectrum with a tail up to more than 100 MeV.

V. CONCLUSIONS

A magnetic spectrometer has been designed and realized for the first step of the PlasmonX project. The experimental setup is still in the commissioning phase. The most challenging goal is to face the high noise laser-plasma interaction environment, suitably screening the electronic readout system. The principle of the detector and the active scintillating fiber screen proved to perform as expected, thanks to an alternative purely optical readout, based on CCD. We are confident to overcome the high noise obstacles in the next commissiong phase and to use with success the planned electronics readout system.

[1] T. Tajima and J.M. Dawson, Phys. Rev. Lett, 43 (1979) 267.
[2] E. Esarey et al., Rev. Mod. Phys. 81(3) (Au 2009) 1229-1285.
[3] L.A. Gizzi et al, Nuovo cim. (2009) C32N3-4:433-436.
[4] R. Faccini et al, Nucl. Instrum. Meth., A 623, 704-708 (2010).
[5] C.Benedetti, A.Sgattoni, P.Tommasini, proceedings of EPAC 2008 pp WEPP127, 23-27, (Jun 2008)
[6] R.Faccini et al, Physics.ins-det/10023497 preprint (2010), submitted to Phys. Instr. Det.
[7] P.Barillon et al, Proc. of Prague 2007, Electronics for particle physics, 26 (2007).
[8] F.Cusanno et al, Nucl. Instr .Meth. A617, 217 (2009).
[9] G. D'Agostini, Nucl. Instr. Meth, A362:487-498, 1994.

[10] Nucl. Instrum. Meth. A515 (2003) 524.